

# Sintering of oxide and carbide ceramics by electron beam at forevacuum pressure

E Dvilis<sup>1</sup>, O Tolkachev<sup>1</sup>, V Burdovitsin<sup>2</sup>, A Khasanov<sup>1</sup>, M Petyukevich<sup>1</sup>

<sup>1</sup>Department of nanomaterials and nanotechnologies, National Research Tomsk Polytechnic University, 30 Lenin Ave., Tomsk, 634050, Russia

<sup>2</sup>Tomsk University of Control Systems and Radioelectronics, 40 Lenin Ave., Tomsk, 634050, Russia

Email: [dvilis@tpu.ru](mailto:dvilis@tpu.ru)

**Abstract.** Novel approaches for electron beam sintering of zirconia and silicon carbide ceramics have been investigated: application of forevacuum pressure plasma-cathode to compensate the charge induced by the electron beam on the green compact surface, and previous dry powder compaction under powerful ultrasound assistance. Dense YSZ ceramics with submicron and micron grains have been consolidated by electron beam sintering after powder compaction using ultrasound.

## 1. Introduction

Electron Beam Sintering (EBS) is a kind of Field Assisted Sintering. However to provide a temperature available for sintering of ceramics it is necessary to use electron beam in high vacuum, and with megaelectronvolt (MeV) energy [1]. Hence, there are significant limitations for wide application of EBS: high power consumption; shielding effect for dielectric materials due to charge accumulation on the sample surface, which leads to deceleration and deflection of the electron beam; formation of micro- and macroscopic defects in sintered ceramics [2].

The specified problem may be resolved by application of the electron beam with energy 5-15 keV in a forevacuum, i.e. in the pressure range of 5-20 Pa. For this purpose the electron beam source is the forevacuum pressure plasma-cathode [3, 4], which provides the generation of dense plasma owing to hollow-cathode discharge. The plasma compensates the charge induced by the electron beam on the dielectric target surface. In this case the floating potential near the target is much less than accelerating voltage and impact of the electron beam on the dielectric ceramics is similar to effect on metals [5].

The aim of the work was to carry out testing of EBS method in forevacuum with electron beam having kiloelectronvolt energy in order to sinter yttrium-stabilized zirconia (YSZ) and silicon carbide (SiC) ceramics.

## 2. Powder compaction and sintering. Experimental techniques

The raw powders were commercial YSZ nanopowder TZ-3YS (TOSOH) with average particle size of 200 nm and commercial SiC powder (Neomat) with average particle size of 1  $\mu\text{m}$ .

To prepare green compacts for EBS the dry powder pressing without any binders and lubricants using both conventional uniaxial compaction and uniaxial compaction under powerful ultrasound assistance (PUA) [6] have been used. Compaction pressure was 480 MPa. In case of PUA compaction the



resonant ultrasound frequency was 21 kHz, power of ultrasonic generator was 4 kW. Green pellets after compaction had the diameter of 14 mm, thickness about 4 mm and green density up to 59%.

Setup of EBS installation is shown in Figure 1. On opposite walls of a vacuum chamber (1) two identical electron guns (2) supplied with focusing and deflecting coils (3) were established. Their heat protection was provided by shields (4). Two identical electron beams (5) from two opposite directions provided uniform heating of green pellet (6), which was located on a graphite crucible (7) in special holder and settled down in the plane of a perpendicular axis of the electron beams. For visual observation through the window (8) two mirrors (9) were mounted in the vacuum chamber. Measurement of a sample temperature was carried out by contactless method using RAYTEK 1MH pyrometer (10).

EBS modes have been varied depending on ceramics type and for purpose of their optimizing. Accelerating voltage of the electron beam  $U$  varied from 10.5 keV to 12 keV; beam current  $I$  was in the range 200 mA – 280 mA. Sintering duration (exposition of green compacts under electron beam at sintering temperature) varied from  $t_e = 5$  sec to  $t_e = 80$  min. EBS energy for sintering  $E$  (MJ) has been calculated by the equation  $E = Ut_e$ .

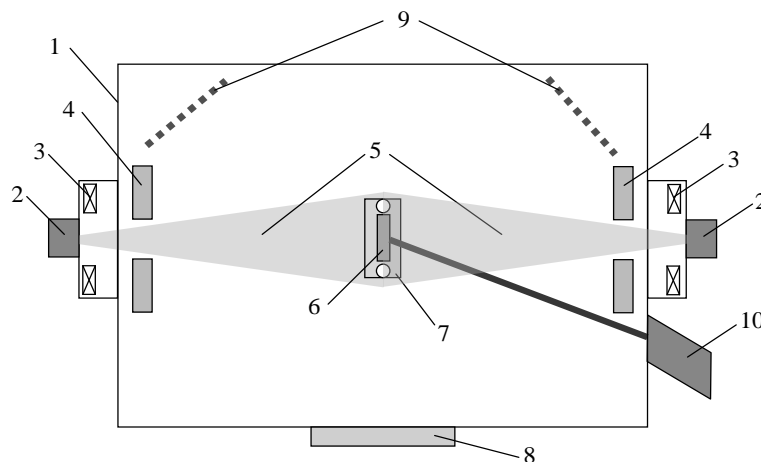


**Figure 1.** Setup of installation for electron beam sintering: 1 – vacuum chamber, 2 – electron guns with the hollow cathode, 3 – focusing and deflecting coils, 4 – heat shields, 5 – electron beams, 6 – green pellet, 7 – graphite crucible, 8 – observation window, 9 – mirrors, 10 – pyrometer.

Also YSZ green pellets have been consolidated by the conventional sintering in air (Nabertherm LHT 02/18 furnace).

The microstructure and mean grain size  $d_g$  versus relative density  $\rho$  of sintered specimens have been examined by SEM analysis (JSM-7500FA JEOL; “ImageJ” code). Phase composition has been studied by XRD analysis (XRD-7000S Shimadzu) and Vickers microhardness by the nanoindentation technique (DUH-211S Shimadzu).

### 3. Results and discussion

#### 3.1. YSZ ceramics

YSZ samples were sintered by EBS at temperature 1400-1450 °C and EBS energy was variable from 5.5 MJ to 12.3 MJ.

For all EBS modes YSZ melting, recrystallization were avoided and XRD analysis shown that sintered samples had pure tetragonal phase of  $ZrO_2$  (Figure 2).

It was found an extreme behavior of the relative density  $\rho$  and grain size  $d_g$  of YSZ ceramics vs EBS energy (Figure 3): at  $E = 8.4$  MJ ( $t_e = 40$  min) mean grain size had maximum value  $d_g \approx 5 \mu\text{m}$ , as well

as maximum density  $\rho = 95\%$  (Figure 4a), but at  $E = 11$  MJ ( $t_e = 60$  min)  $d_g$  was significantly decreased down to  $2.5 \mu\text{m}$ , however density remains high, about  $\rho = 95.2\%$ . Following increasing EBS energy leads to lower  $\rho$  and  $d_g$  values. This behavior indicates an opportunity of optimization of the EBS modes to achieve the higher YSZ density at lower mean grain size.

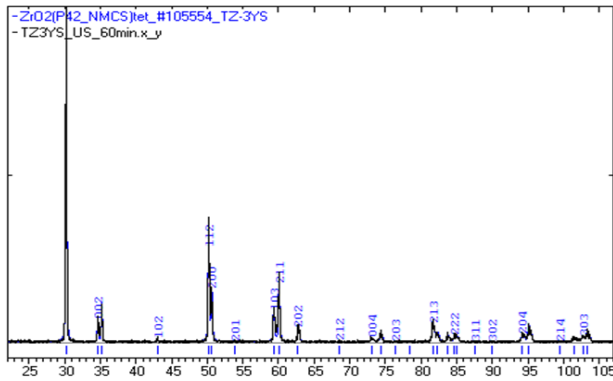


**Figure 2.** XRD pattern of YSZ ceramics sintered by EBS technique.

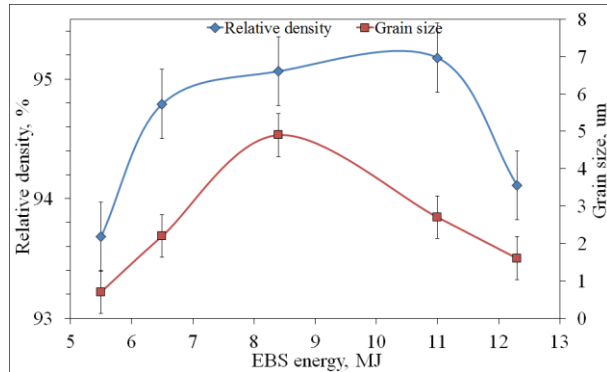


**Figure 3.** Relative density and grain size of YSZ ceramics vs EBS energy.

Conventional sintering ( $1400^\circ\text{C}$ , 60 min) showed  $\rho = 97\%$ , but large grain size  $d_g = 22 \mu\text{m}$ . EBS after conventional uniaxial pressing and after compaction under PUA showed that in case of PUA density can be achieved up to  $97.3\%$  and compaction modes influence on the grain size. EBS at  $t_e = 5$  sec after conventional pressing leads to  $d_g = 4.8 \mu\text{m}$ , but at  $t_e = 60$  min the mean grain size was  $1.5 \mu\text{m}$ . The same EBS modes, but after PUA compacting, provided  $d_g = 2.4 \mu\text{m}$  and submicron grain scale of  $0.7 \mu\text{m}$  correspondingly.

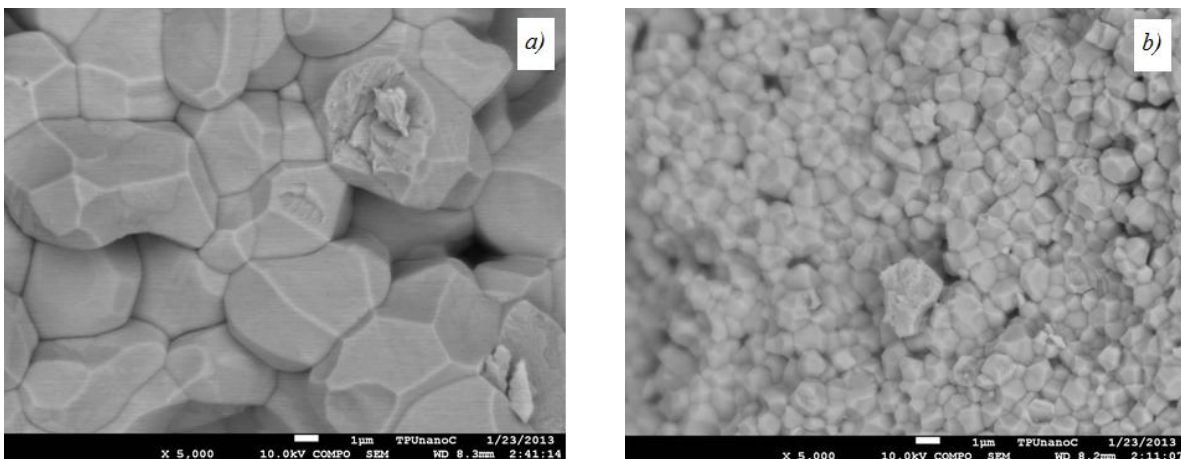


**Figure 4.** Microstructure of YSZ ceramics (a) after EBS at  $E = 8.4$  MJ; (b) after EBS at  $E = 5.5$  MJ.

Microhardness of YSZ ceramics consolidated by EBS after conventional pressing was  $13.7$  GPa, but after PUA compacting at the same EBS modes it was increased up to  $15.9$  GPa. So it was shown a possibility to decrease YSZ mean grain size at high density and increase the microhardness by application of dry powder compaction under powerful ultrasound assistance.

Important peculiarity of YSZ ceramics microstructure after EBS is presented in Figure 5: the porous surface layer with thickness of about 11  $\mu\text{m}$  and mean pore size comparable with  $d_g$ .

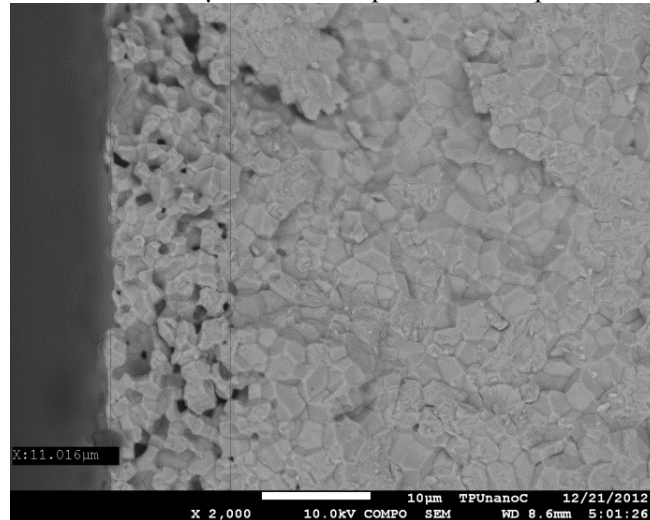


**Figure 5.** Porous surface of the YSZ ceramics after EBS.

Formation of this porous surface can be explained by the modeling of YSZ consolidation by EBS using the assumption of anisotropic sintering due to electron charge accumulation on the surface grains. Such charging leads to slowing down of sintering in normal direction to the surface. Figure 6a shows the surface model of initial green compact with monolayers (S3D-Evolution code, Smartimtech) and Figure 6b, 6c - simulation of anisotropic sintering and porous space of sintered ceramics, having satisfactory correlation with the SEM image of YSZ ceramics after EBS (Figure 6d).

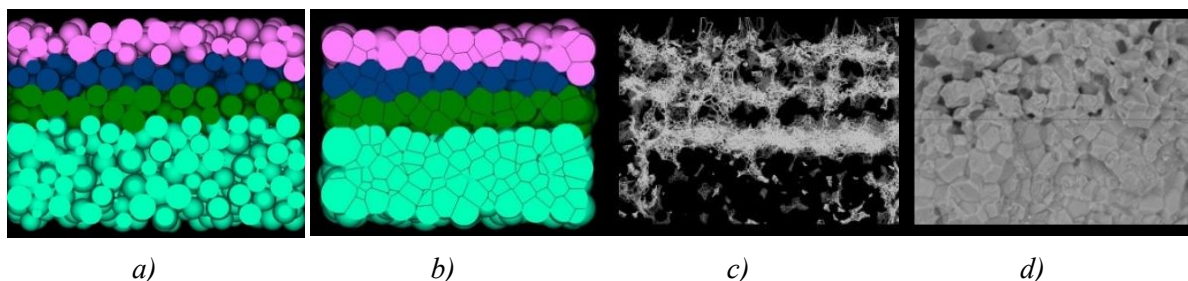


**Figure 6.** Simulation of anisotropic sintering (*a*, *b*), porous space (*c*) and SEM image of YSZ ceramics after EBS (*d*).

### 3.2. SiC ceramics

EBS of SiC green pellets in a range from 1700  $^{\circ}\text{C}$  to 1950  $^{\circ}\text{C}$  demonstrated the mass loss (ablation) and density decreasing even at slight shrinkage (Figure 7). The possible reason of such behavior is additional Joule heating in SiC owing to relatively high specific resistance at EBS temperature 1700  $^{\circ}\text{C}$  (5  $\Omega\cdot\text{cm}$ ) in comparison with specific resistance of YSZ at 1400  $^{\circ}\text{C}$  (1  $\Omega\cdot\text{cm}$ ).

Different microstructure of sintered SiC samples along their spall and pellet surface has been found by the SEM analysis (Figure 8a-d) which can be explained by nonuniform distribution of EBS temperature from the pellet center to edge due to nonuniform Joule heating.

Thus, more thorough research is essential for optimization of EBS modes in order to sinter dense SiC ceramics.

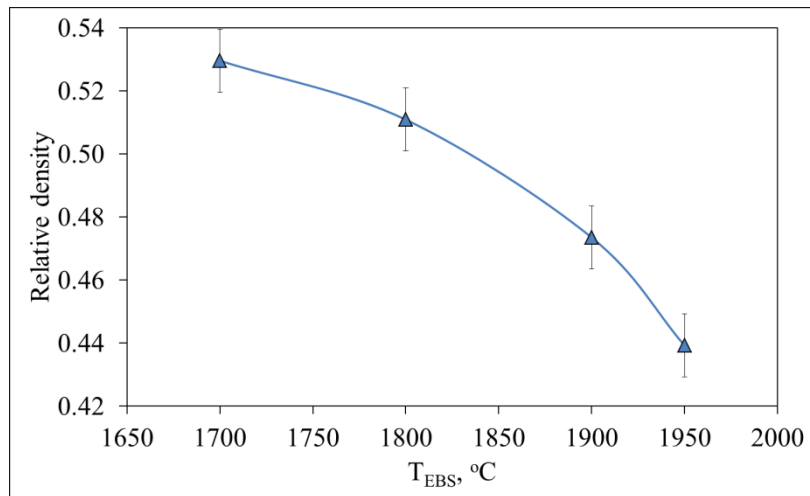


**Figure 7.** Porous surface of the YSZ ceramics after EBS.

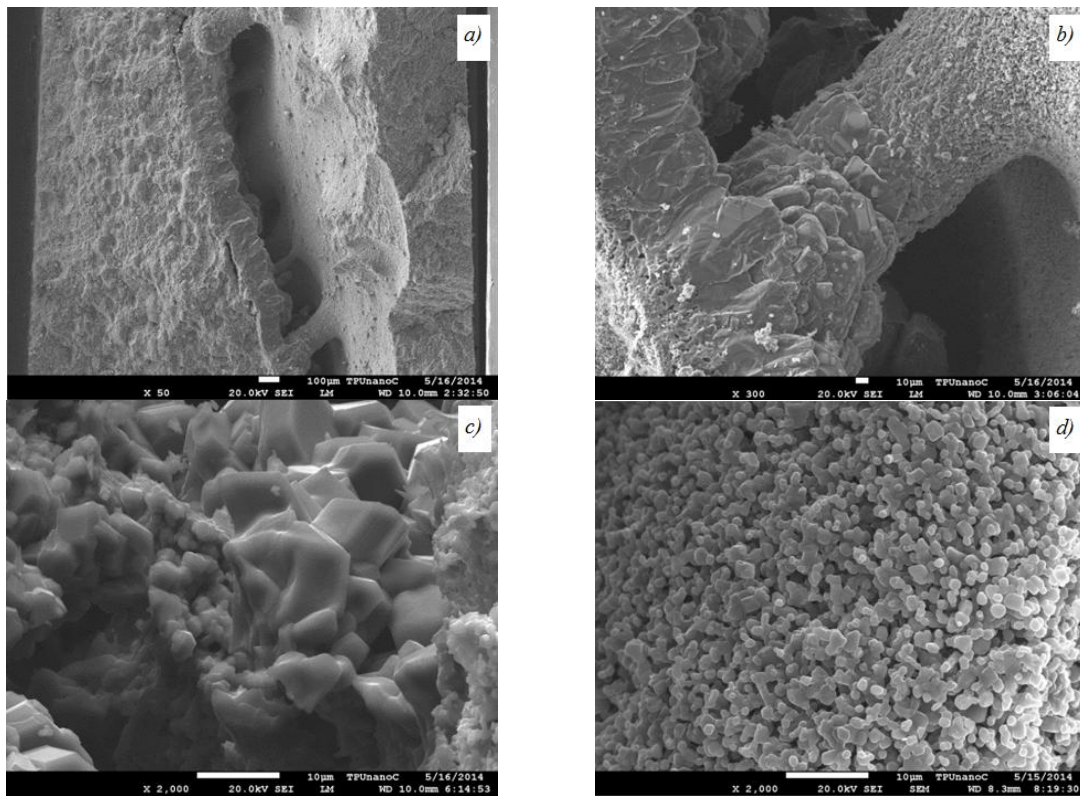


**Figure 8.** Microstructure of ceramics: (a) cavities in the SiC sample spall after EBS due to ablation; (b) cavities in the central area of pellet surface; (c) SiC recrystallized junctions in necks in the central area of pellet surface; (d) small SiC grains in the edge area of pellet surface.

#### 4. Conclusions

1. Electron beam sintering in forevacuum can be effective method to sinter dense YSZ ceramics with small grains. Submicron grain scale can be achieved using EBS at exposition duration 60 min after dry YSZ nanopowder compaction under powerful ultrasound assistance.

2. Porous surface layer on the YSZ ceramics can be caused by anisotropic sintering.
3. EBS of SiC ceramics is accompanied by the ablation due to high SiC specific resistance.

### Acknowledgements

The work has been supported by the RFBR grant No.14-08-00775, State assignment "Science" and FTP project #RFMEF157514X0003.

### References

- [1] Annenkov Yu M 1996 *Russian Physics Journal* **39** 1146-59
- [2] Sun C N, Gupta Mool C and Karen M B 2010 *J. Am. Ceram. Soc.* **93** 2484–6.
- [3] Burdovitsin V A and Oks E M 2008 *Laser and particle beams*, **26** 619–35.
- [4] Burdovitsin V, Dvilis E., Zenin A, Klimov A, Oks E, Sokolov V and Kachaev A 2014 *Advanced Materials Research* **872** 150-6
- [5] Burdovitsin V, Klimov A and Oks E 2009 *Technical Physics Let.* **35** 511-3
- [6] Khasanov O L and Dvilis E S 2008 *Adv. Appl. Cer.* **107** 135-41
- [7] Munro R G 1997 *J. Phys. Chem. Ref. Data.* **26** 1195-1203